Distributed Average Integral Secondary Control for Modular UPS Systems based Microgrids

Wei, Baoze; Gui, Yonghao; Marzabal, Albert; Trujillo, Santi; Guerrero, Josep M.; Vasquez, Juan C.

Published in:
IEEE Transactions on Power Electronics

DOI (link to publication from Publisher):
10.1109/TPEL.2018.2873793

Publication date:
2019

Document Version
Accepted author manuscript, peer reviewed version

This article has been accepted for publication in a future issue of this journal, but has not been fully edited. Content may change prior to final publication. Citation information: DOI 10.1109/TPEL.2018.2873793, IEEE Transactions on Power Electronics

Distributed Average Integral Secondary Control for Modular UPS Systems based Microgrids

Baoze Wei, *Member, IEEE*, Yonghao Gui, *Member, IEEE*, Albert Marzàbal, Santi Trujillo, Josep M. Guerrero, *Fellow, IEEE*, and Juan C. Vásquez, *Senior Member, IEEE*

***Abstract*— This paper presents a distributed average integral secondary control (DAISC) method for modular uninterruptible power supply (UPS) systems based microgrids. For each UPS unit, the local primary control level encompasses droop control and virtual impedance loops, which is commonly used in parallel inverter systems. In order to provide a fast voltage recovery performance, along with excellent power sharing capability among the parallel UPS modules, a distributed secondary control method based on CAN communication is proposed. In a sharp contrast to the existing distributed secondary control strategies, in which the output voltage and frequency of the modules are not shared through the CAN bus, in the proposed apporach the inverter modules of the modular UPS share the integral output value of the secondary controller. By using the proposed novel DAISC approach, a better dynamic power sharing performance along with an inherent anti-windup capability of the integral controller is achieved. Simulation results using PLECS and experiments from a modular UPS platform have been developed to verify the feasibility and effectiveness of the proposed distributed secondary control. The results shown that good performance of voltage recovery and power sharing of the proposed control method is obtained.**

***Index Terms*— distributed secondary control, CAN bus, modular UPS, virtual impedance, droop control, parallel inverters, power sharing.**

I. INTRODUCTION

The concept of microgrid (MG) is becoming more important to meet the requirement of the increasing penetration of renewable energy sources from distributed generators (DGs) into utility grid or supplying distributed loads [1] [2]. Typically it consists several DGs working in parallel in an MG. Different kinds of control methods have been proposed for the control of an MG, they are mainly classified into centralized, decentralized, distributed, and hierarchical control methods [3]–[11].

In this sense, uninterruptible power supply (UPS) systems are widely used for the critical loads like data center that cannot afford power loss, which are also suitable to create highly reliable microgrids [12], [13]. In order to improve the availability and reliability of a UPS system, the modular UPS concept appeared at later 1990s [13]. A modular UPS contains several converter modules working in parallel to feed power to the loads connected to an MG, often called *critical bus*. So that salient control concepts in MGs can be transferred to the control modular UPS systems [14]-[17].

The modular UPS's has some advanced features, such as easy scale of rated power by increasing the power capacity regardless of the rating limited of switching devices; easy to install and maintain service. The feature of *plug and play* makes it more convenient to repair or replace damage modules without powering-off the whole system (also named *hot-swap* operation), which can increase the flexibility, reliability and maintainability of power supply systems to meet the requirements of customers. Further, the redundant power modules in the UPS system can ensure higher availability: when one power module fails, another one can take over quickly to make guarantee the electricity supply to the loads [13], [15].

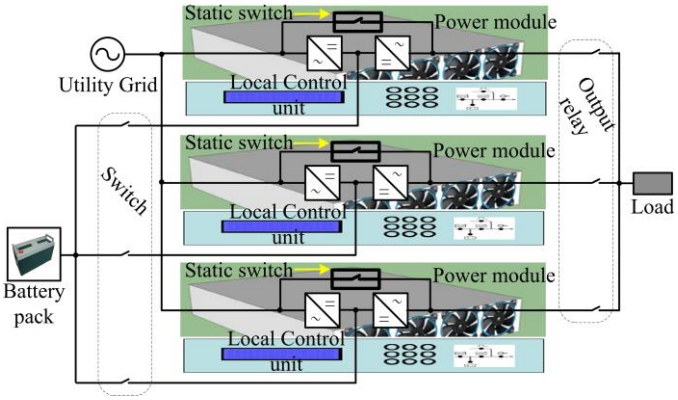

Fig. 1. Structure of a modular UPS system.

As abovementioned, like some DGs in an MG, in a modular UPS, the converter modules operate connected in parallel with each other. Some technical objectives may be obtained by using proper control strategies, such as voltage and frequency regulation, and average active/reactive power sharing among parallel modules [18]. Thus, proper control strategies are essential to guarantee the proper and stable operation [18]-[20]. As an advanced control method, the hierarchical control architecture can be applied to modular UPS system control to endow high-level of system reliability [3], [5], [21]-[23].

In the hierarchical control, it mainly contains three levels, named primary, secondary, and the tertiary control levels [23]-[26]. The primary control is the local fundamental level that operates on a fast timescale and maintains both voltage and frequency stability of the system while keeping active/reactive

This article has been accepted for publication in a future issue of this journal, but has not been fully edited. Content may change prior to final publication. Citation information: DOI 10.1109/TPEL.2018.2873793, IEEE Transactions on Power Electronics

power sharing. The control framework consisting of the droop method plus a virtual impedance loop is widely adopted for the primary level [27]-[31]. Unfortunately this framework, achieves good levels of power sharing by degrading frequency and voltage amplitude regulation [24], [26], so that a secondary control is applied to compensate the voltage and frequency deviations [32], [33]. Further, the secondary control has been recently expanded to endow some additional functions such as voltage unbalance compensation, average power sharing improvement, and so on [31], [34]. Finally, the tertiary control is responsible for power management concerning the economic optimization of a system [24], [26], which is out of scope of this paper.

The control method discussed in this paper is applied to a modular UPS system. The voltage and frequency restoration occupies an important position in the control scheme, and this paper mainly discusses the secondary control level for the modular UPS system. Many methods have been proposed to address this issue by using a centralized secondary control [35], [36] that requires complex communication links for huge amounts of data transmission and may suffer from a single point-of-failure [24].

In order to have a similar performance with the centralized control, but overcoming its drawbacks, distributed control concepts have been brought into the secondary control level [1], [9], [10], [11], [21], [22], [24], [25], [37]. However, most of the research works appearing in the literature mainly discuss communication network structure and data sharing among the converter modules or DGs. Some of the proposed algorithms for distributed secondary control are consensus-based [22]. The reason of this is that for the existing distributed control strategies, the data shared through the network is mainly the voltage and frequency information of each module. The diagram of the secondary control itself never changes in a wired communication system, so that the difference remains in the scheme of data sharing network. Of course, the network is important for the reliability of the distributed secondary control, but this paper will focus on the distributed secondary control itself from a different angle.

Alternatively, in [37], a general distributed networked secondary control is presented, and in the control scheme, each local controller will collect voltage and frequency information from all the other controllers through the network and then get the average value of them, which will be used to compare with voltage and frequency references in their own secondary control loop. However, by using the conventional distributed secondary control method in [37], after a disconnection and a subsequent connection of a module, the power cannot be averagely shared again, and the output power of the reconnected module is much lower than the others. It means that the secondary control cannot guarantee power sharing after this operation is performed since the power modules cannot recover to the same operation point. This is the main motivation to develop the new distributed secondary control proposed in this paper.

In order to solve the problem of the conventional distributed secondary control structure like the one shown in [37], a distributed averaging integral secondary control (DAISC) based on low bandwidth CAN communication is proposed in this paper. The communication network used in this work is as the same as in [37], but compared with the conventional distributed secondary control structure, the difference is that, in the proposed method, the voltages and frequencies of each module are not shared, since the proportional integral (PI) controller is often adopted in the secondary control loop to eliminate the steady state error, then the output value of the integral part of the secondary controller is the one to be sent to the network. Once all the modules receive these information, an average value of the integral controller will be used to replace the local integral output value and add with the proportional part to get the final output. With the DAISC, at any time one can guarantee that each module can recover the voltage and frequency immediately during the dynamic condition, and the important contribution is that the average power sharing performance is also improved. Another advantage is that since the integral part of the PI controller is always shared among the modules, there is an inherent anti-windup capability with the improved secondary control.

To verify the effectiveness of the proposed control method, simulations with PLECS and experiments on a modular UPS platform have been implemented. With the DAISC, the average power sharing performance can always be obtained even after connect or disconnect inverters from the microgrid, which is an important issue to be considered for the modular UPS.

This paper is organized as follows. In Section II, the concept of the conventional distributed secondary control proposed in [37] is briefly introduced first, and some simulation results are presented for performance verification and problem formulation. Then the idea of the proposed DAISC is discussed in Section III, and the stability analysis of both voltage and frequency is provided, as well as the power sharing performance is discussed. In Section IV, simulation results with several dynamic tests are presented using the DAISC. In Section V, experimental results are implemented with a real modular UPS platform. The conclusions are given in Section VI.

II. Problem Formulation

The conventional *P-f/Q-E* droop functions are suitable for parallel inverters when there is highly inductive output impedance, which is common when using *L* or *LCL* filters [38], [39]. However, considering the project discussed in this paper, the UPS system use *LC* filters and low voltage lines are predominantly resistive. Thus, in order to keep consistency, resistive virtual output impedance is here selected, which can also reduce mathematical transformation compared to adding virtual inductance [40], [41]. For such a case, the droop functions with secondary control can be expressed as follows [14]:

$$E_i = E^* - m_p P_i + \delta_{Eisec} \quad (1)$$

$$f_i = f^* + m_q Q_i + \delta_{fisec} \quad (2)$$

where f^* and E^* represent the frequency and voltage amplitude references, m_p and m_q are the droop coefficients, and δ_{fisec} and δ_{Eisec} are the secondary frequency and voltage amplitude restoration terms. The active power P_i can be controlled by the inverter output-voltage amplitude while the reactive power Q_i can be regulated by the inverter frequency, which is the

This article has been accepted for publication in a future issue of this journal, but has not been fully edited. Content may change prior to final publication. Citation information: DOI 10.1109/TPEL.2018.2873793, IEEE Transactions on Power Electronics

opposite strategy of the conventional droop [38]. More details about the choice of droop functions and the analysis of output impedance can be found in [3], [14], [38]-[43]. The reactive power Q_i is related to the frequency, which is a global variable, being easier to control with the primary control; while the active power P is regulated by the voltage, which is a local variable, hence more difficult to control. Hence, in this paper is mainly focusing on the active power sharing performance.

A. *The concept of the conventional distributed secondary control*

Fig. 2 shows the control diagram of the conventional distributed secondary control [37]. In this control method, the output voltages of all the inverters are shared through a communication bus (in our case we choose the CAN bus), and then every unit will calculate the average voltage and compare with the reference voltage by using a local PI controller in order to get the voltage compensation value $\delta_{Ei\sec}$. By the same principle, the frequency compensation value $\delta_{fi\sec}$ from the distributed secondary control can also be obtained. The secondary controllers can be expressed as:

$$\begin{aligned}\delta_{E_{i\sec}} &= K_{PE\sec}\left(E_{ref}-E_{av}\right)+\frac{K_{IE\sec}}{s}\left(E_{ref}-E_{av}\right)\\ \delta_{f_{i\sec}} &= K_{Pf\sec}\left(f_{ref}-f_{av}\right)+\frac{K_{If\sec}}{s}\left(f_{ref}-f_{av}\right)\end{aligned}, \quad (3)$$

where

$$\begin{aligned}E_{av} &= \frac{1}{n}\sum_{i=1}^{n}E_i\\ f_{av} &= \frac{1}{n}\sum_{i=1}^{n}f_i\end{aligned}. \quad (4)$$

where E_{ref} and f_{ref} are the references of voltage and frequency, respectively. E_i and f_i are the voltage amplitude and frequency of the i-th module, respectively; $K_{PE\sec}$ and $K_{IE\sec}$ are the proportional and integral coefficients of the voltage secondary controller, respectively; $K_{Pf\sec}$, and $K_{If\sec}$ are the coefficients of the frequency secondary controller.

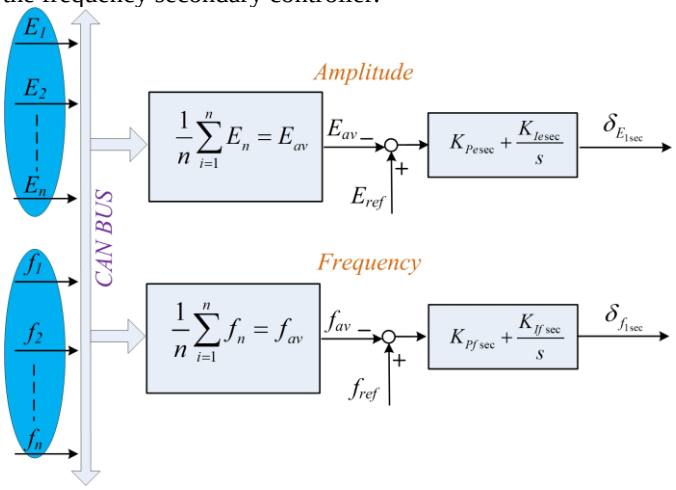

Fig. 2. The conventional distributed secondary control scheme.

B. *The performance verification and problem expression of the traditional distributed secondary control*

In order to verify the performance of the conventional distributed secondary control, simulation has been implemented. Fig. 3 shows the control diagram for the parallel operation of a number of n power modules in a modular UPS system using the droop, virtual impedance and distributed secondary control. Fig. 4 depicts the communication configuration for the distributed secondary control. When applying the conventional distributed secondary control, the power module will send voltage and frequency information to the communication link only if the module is delivering power to the load, it means only the modules operate in parallel to support the load will communicate with each other. Consequently, if a power module is disconnected without delivering power to the load, it should stop sending voltage and frequency information to the communication link since it is not part of the paralleled system anymore.

The simulations were implemented by using PLECS. In order to mimic accurately the experimental hardware, a switching model was built in the simulation, and the whole control scheme was implemented using C language, similar to the code used in the digital signal processor (DSP) unit of the real modular UPS platform.

For the implementation of conventional distributed secondary control, the simulation was configured as: before 0.15s, two inverter modules were connected to the load and delivering power to the load; then at 0.15s, the module #2 was disconnected from the load and at 0.25s, it was reconnected to the load again. Before 0.15s and after 0.25s, the two modules were communicated to exchange voltage and frequency information for the secondary control, the difference is that during the time 0.15s to 0.25s the communication for data exchange among the two modules was stopted, because the module #2 was disconnected from the load without delivering power. In other words, these two modules were not working in parallel during this time , so that they would use their own voltage and frequency information, while the voltage and frequency information from a module which is not delivering power to the load should not participate in the control of the rest of other parallel-connected modules.

From the simulation results shown in Fig. 5, it can be seen that, before 0.15s, the output currents can be averagely shared in the two modules, but after 0.25s, the output current of the module #2 was much lower than the other module. One can conclude that the conventional distributed secondary control method is not applicable for the modular UPS system. With the same initial conditions, the secondary control is operated well before 0.15s. However, for the UPS system, each module has their own local control unit; hence, after reconnection at 0.25s, the initial condition of the reconnected converter is different with the one that is still providing power to the load. Hence, due to such a different initial values, each converter converges to a different operating point as shown in Figs. 5-7. Fig. 6 shows the active and reactive power of the two modules in the test, showing that before 0.15s, the power can be averagely shared among two modules. However, after 0.25s when the module #2 was reconnected, the active power cannot be averagely shared.

This article has been accepted for publication in a future issue of this journal, but has not been fully edited. Content may change prior to final publication. Citation information: DOI 10.1109/TPEL.2018.2873793, IEEE Transactions on Power Electronics

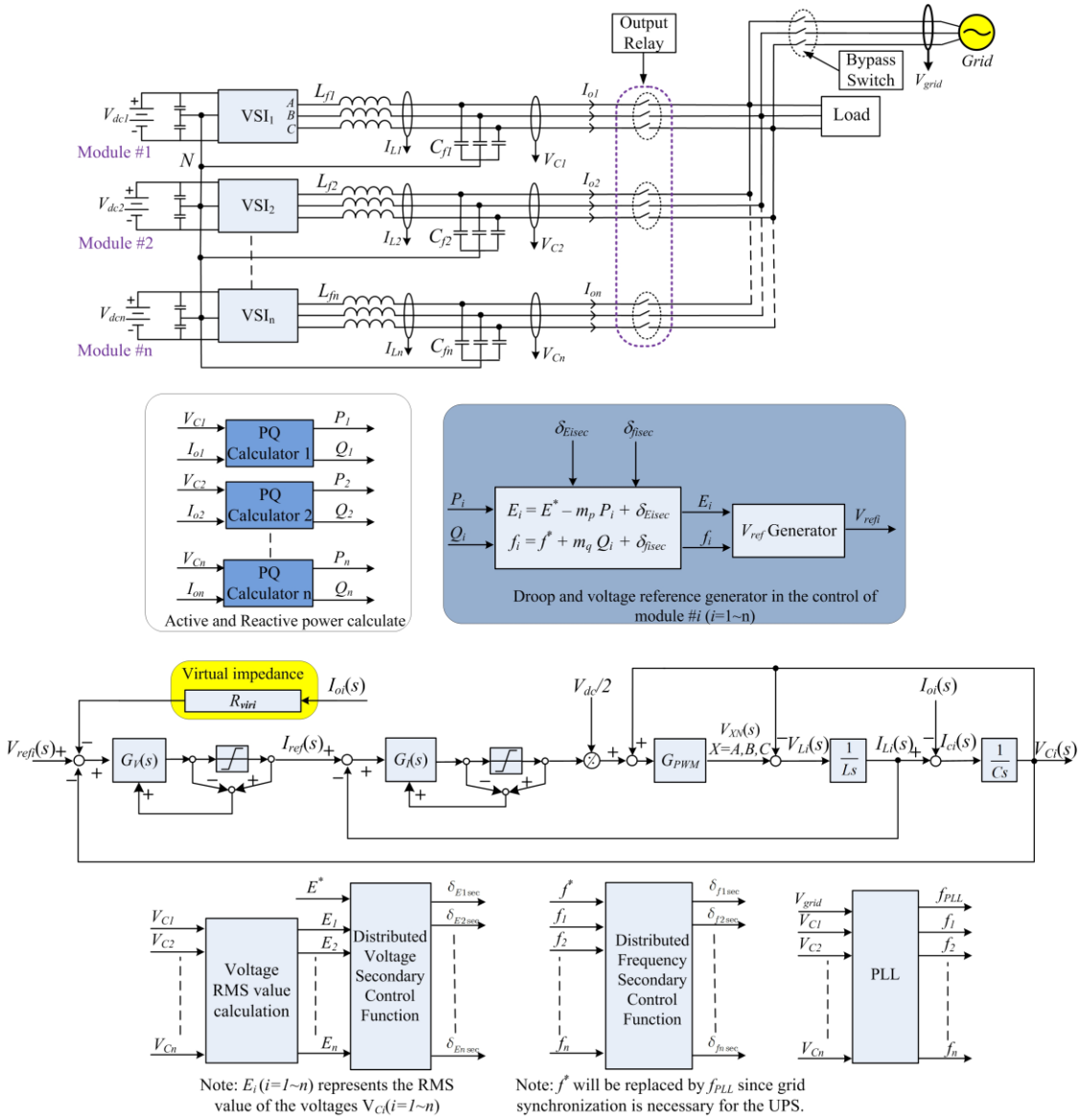

Fig. 3. Control diagram of n parallel modules using droop, virtual impedance and secondary control.

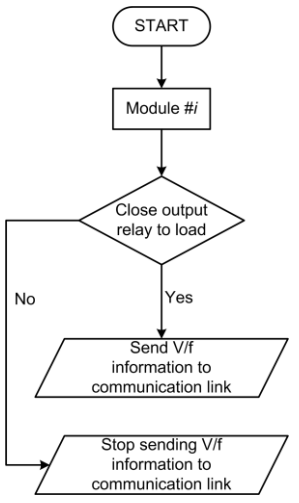

Fig. 4. Data communication setup for the distributed secondary control.

From Fig. 7, the outputs of the secondary control were different from 0.15s and cannot return to the same point at 0.25s, that is because the output voltage of the module #2 was already equal to the reference. It means that the secondary control already finished its work, to recover the voltage, but the power sharing is none of its business. The conventional secondary control cannot ensure that the output voltages of all the parallel-connected modules converge to the same reference voltage under dynamic condition, thus the average power sharing performance is not guaranteed, which is important for the modular UPS. Hence in this paper, a new distributed secondary control is proposed, which can not only recover the voltage and frequency of the parallel power modules but also provide an excellent power sharing performance.

This article has been accepted for publication in a future issue of this journal, but has not been fully edited. Content may change prior to final publication. Citation information: DOI 10.1109/TPEL.2018.2873793, IEEE Transactions on Power Electronics

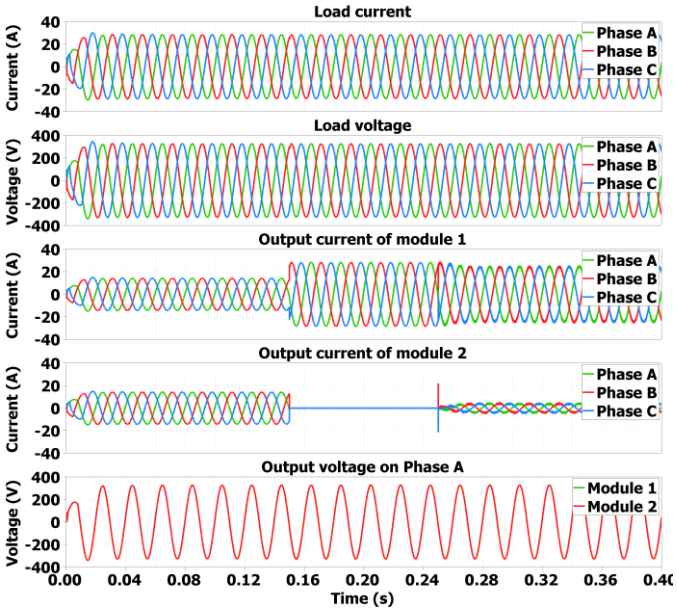

Fig. 5. Simulation results of the two parallel modules.

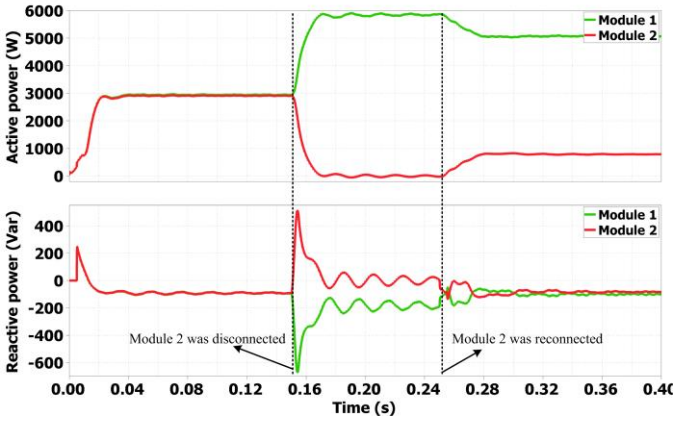

Fig. 6. Phase A active and reactive power of the two parallel modules.

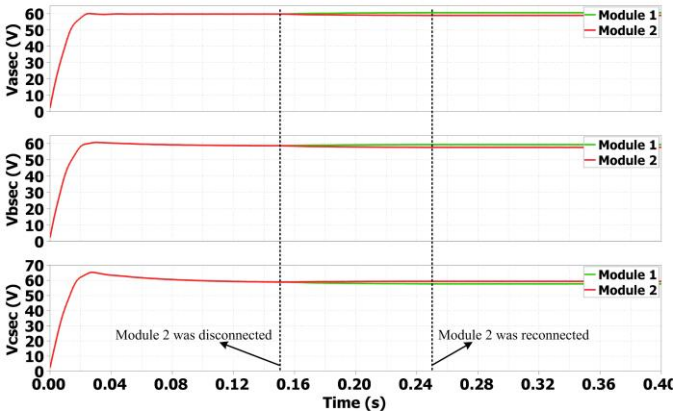

Fig. 7. The three-phase output value of the secondary control of the two parallel modules

III. THE PROPOSED DAISC

In this section, the detail of the proposed DAISC is presented. Stability analysis for both voltage and frequency is provided. In addition, the power sharing performance is discussed based on the stability analysis.

A. *Distributed averaging integral secondary control* (*DAISC*)

In order to improve the dynamic performance on both active and reactive power sharing of the conventional distributed secondary control, the distributed averaging integral secondary control is proposed. Different from the general distributed secondary control, the voltage and frequency information is not shared, instead, the integral part of the secondary control is shared through the communication link, and then the averaged integral value of the secondary control is added to the proportional part to generate the final voltage and frequency compensation values. The principle of the DAISC for voltage control is expressed as follows:

$$\begin{aligned} E_i &= E_{ref} - m_p P_i + \delta_{Ei\sec} \\ \delta_{Ei\sec} &= K_{PE\sec}\left(E_{ref} - E_i\right) + \delta_{E_{I\sec av}} \\ \delta_{E_{I\sec av}} &= \frac{1}{n}\sum_{i=1}^{n}\delta_{E_{Ii\sec}} \quad , (i=1\sim n) \\ \delta_{E_{Ii\sec}} &= \frac{K_{IE\sec}}{s}\left(E_{ref} - E_i\right) \end{aligned} \tag{5}$$

where $\delta_{Ei\sec}$ is the secondary control output of voltage of the *i*-th module, $\delta_{E_{I\sec av}}$ is the averaged integral value of the voltage secondary control loop of all the modules, and $\delta_{E_{Ii\sec}}$ is the integral value of voltage secondary control of the *i*-th module. The DAISC for frequency is proposed as follows:

$$\begin{aligned} f_i &= f_{ref} + m_q Q_i + \delta_{fi\sec} \\ \delta_{fi\sec} &= K_{Pf\sec}\left(f_{ref} - f_i\right) + \delta_{f_{I\sec av}} \\ \delta_{f_{I\sec av}} &= \frac{1}{n}\sum_{i=1}^{n}\delta_{f_{Ii\sec}} \quad , (i=1\sim n) \\ \delta_{f_{Ii\sec}} &= \frac{K_{If\sec}}{s}\left(f_{ref} - f_i\right) \end{aligned} \tag{6}$$

where $\delta_{fi\sec}$ is the secondary control output of frequency of the *i*-th module, $\delta_{f_{I\sec av}}$ is the averaged integral value of the frequency secondary control loop of all the modules, and $\delta_{f_{Ii\sec}}$ is the integral value of frequency secondary control of the *i*-th module. The block diagram of the DASIC is shown in Fig. 9. Totally different from the conventional distributed secondary control, the integral part of the local secondary controller will be sent to the CAN bus to obtain an average value of the integral part. Then it will be added to the proportional part of local secondary control to get the final voltage and frequency compensation value.

By the improvement, once the local integral part of secondary control is sent to the communication link, it will always be equal to the average integral value, the windup will never happen. From the simulation results, along with the performance of average power sharing, an anti-windup capability is also obtained.

This article has been accepted for publication in a future issue of this journal, but has not been fully edited. Content may change prior to final publication. Citation information: DOI 10.1109/TPEL.2018.2873793, IEEE Transactions on Power Electronics

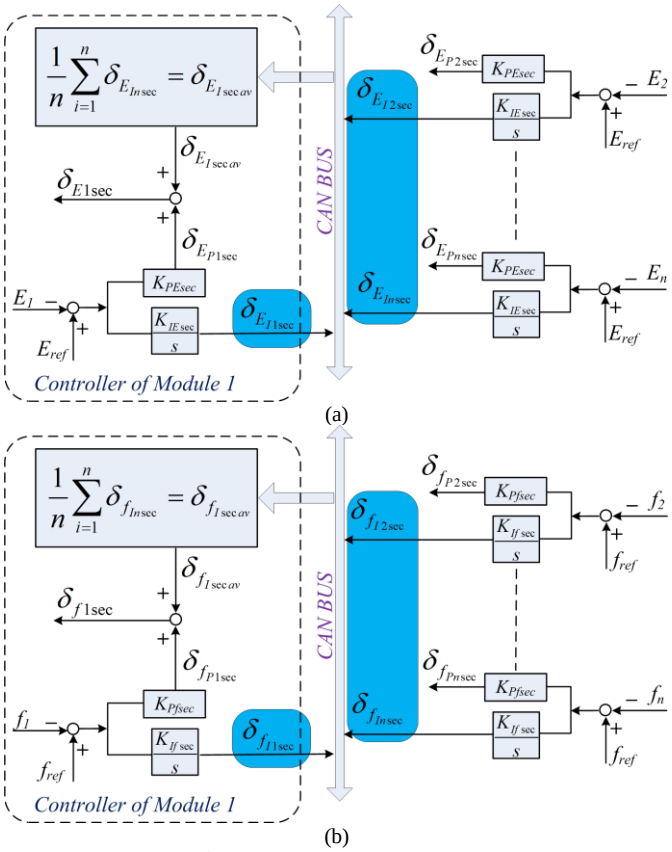

Fig. 8. Block diagram of the proposed DAISC. (a) Voltage secondary control (b) Frequency secondary control.

B. *Stability analysis of voltage considering the secondary control*

In order to discuss the influence of the proposed DAISC to the system, stability analysis is presented. Since in the droop and the secondary control, the voltage and frequency are controlled separately based on the approximation that voltage is mainly dependent and regulated by active power, while the frequency is mainly dependent and regulated by reactive power under the case of resistive output impedance [38], [39], [42], [43]. Thus, for simplicity, the analysis of voltage and frequency can be done separately, which also appears in [44], [45]. To avoid unnecessary technical complications, a model without any delay in adjusting the output voltage with a simple low-pass filter is used[44]:

$$\dot{E}_i = E_{ref} - E_i - m_p P_i + \delta_{Ei\sec}. \tag{7}$$

The active power injection at the *i*-th module takes the form [46]:

$$P_i = E_i I_{oi} \cos\phi \tag{8}$$

where I_{oi} is the output current of *i*-th module. Normally, the power angel ϕ is a small value especially when a resistive output impedance is obtained, thus $\cos\phi \approx 1$ is adopted [46]. Then (12) can be rewritten as $P_i \approx E_i I_{oi}$. To simplify the stability analysis, we show the case of two modules as $n = 2$. From (5), (7), and (8), we can obtain a dynamic system model as follows:

$$\begin{aligned}
\dot{E}_1 &= (1+K_{PE\sec})E_{ref} - (1+K_{PE\sec}+m_P I_{o1})E_1 + \delta_{E_{I\sec av}} \\
\dot{E}_2 &= (1+K_{PE\sec})E_{ref} - (1+K_{PE\sec}+m_P I_{o2})E_2 + \delta_{E_{I\sec av}} \\
\dot{\delta}_{E_{I\sec av}} &= [K_{IE\sec}(E_{ref}-E_1) + K_{IE\sec}(E_{ref}-E_2)]/2
\end{aligned} \tag{9}$$

Let us define $e_1 = E_1 - E_{ref}$ and $e_2 = E_2 - E_{ref}$. If we define a state $x_E = \begin{bmatrix} e_1 & e_2 & \delta_{E_{I\sec av}} \end{bmatrix}^T$ and an input $u_E = \begin{bmatrix} m_p E_{ref} I_{o1} & m_p E_{ref} I_{o2} \end{bmatrix}^T$, then the system (7) is changed into a linear system

$$\dot{x}_E = A_E x_E + u_E, \tag{10}$$

where

$$A_E = \begin{bmatrix} -1-K_{PE\sec}-m_p I_{o1} & 0 & 1 \\ 0 & -1-K_{PE\sec}-m_p I_{o2} & 1 \\ -K_{IE\sec}/2 & -K_{IE\sec}/2 & 0 \end{bmatrix}.$$

We only consider $\dot{x}_E = A_E x_E$. If all eigenvalues of A_E are negative, then the system is stable, that is, $E_{1,2}$ converge to E_{ref}. It is hard to check if A_E has all negative eigenvalues in the whole operating range. Consequently, in this study we will use Lyapunov theorem [47]. Let's consider a Lyapunov function candidate as follows:

$$V_{E,lyap} = \frac{1}{2}e_1^2 + \frac{1}{2}e_2^2 + \frac{1}{K_{EI\sec}}\delta_{E_{I\sec av}}^2. \tag{11}$$

The time derivative of (11) can be expressed as follows:

$$\dot{V}_{E,lyap} = -(1+K_{PE\sec}+m_p I_{o1})e_1^2 - (1+K_{PE\sec}+m_p I_{o2})e_2^2. \tag{12}$$

If K_{PEsec}>-1-$m_p I_{o1}$, and K_{PEsec}>-1-$m_p I_{o2}$, then (12) is negative semi-definite, which means $E_{1,2}$ converge to E_{ref}. Thus, from (9), $\dot{\delta}_{E_{I\sec av}} \equiv 0$, which means that $\delta_{E_{I\sec av}}$ is also stabilized based on LaSalle's theorem [47].

Consequently, the system (10) is stable. In addition, for this modular UPS project, the output current is always higher or equal to zero since it is unidirectional, thus the system will be stable if K_{PEsec}>-1. In order to further analyze the system, by considering the control parameters used in the simulation and experiments, we draw the traces of the eigenvalues of A_E when various secondary control parameters are selected, which are shown in Fig. 9. The control parameters used in the simulation and experimental tests are listed in Table I. From Fig. 9, we can conclude that with the proposed control and the selected parameters, we can guarantee stability of the system.

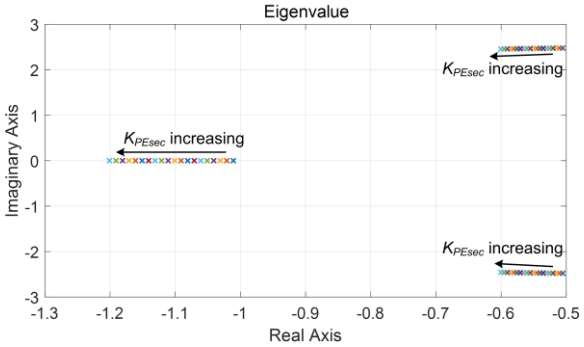

(a)

This article has been accepted for publication in a future issue of this journal, but has not been fully edited. Content may change prior to final publication. Citation information: DOI 10.1109/TPEL.2018.2873793, IEEE Transactions on Power Electronics

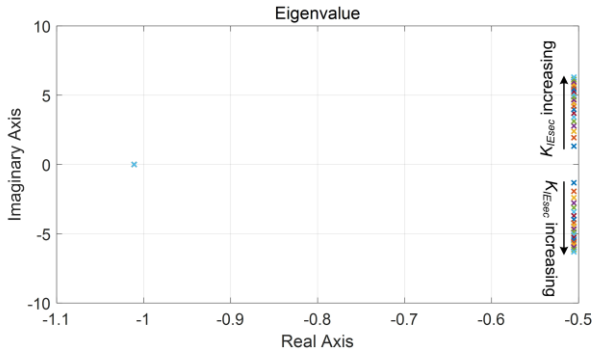

(b)

Fig. 9. Eigenvalues traces of the system (9) (a) for K_{PEsec} if various from 0.01 to 0.2, (b) for K_{IEsec} is various from 1 to 20.

C. Stability analysis of frequency considering the secondary control

Since the frequency secondary control is using the same principle as the voltage, thus a similar model can be written as:

$$\dot{f}_i = f_{ref} - f_i + m_q Q_i + \delta_{fi\sec}. \tag{13}$$

The reactive power injection at the *i*-th module takes the form [46]:

$$Q_i = -E_i I_{oi} \sin\phi. \tag{14}$$

According to [46], the power angel is obtained as $\phi = \Delta\omega\Delta t$, $\Delta\omega = 2\pi(f_i - f_{ref})$, $\Delta\omega$ is the frequency difference between the inverter output voltage frequency f_i and the reference frequency f_{ref} for the common bus voltage, which is the common point of the power modules at the load side in this paper. As discussed in the former section, the power angle is small, then (14) can be rewritten as $Q_i \approx -E_i I_{oi}\phi$. Thus, similar to the voltage, when considering two modules in the UPS system, we can obtain a dynamic system model as follows:

$$\begin{aligned}
\dot{f}_1 &= (-1 - K_{Pf\sec} - 2\pi m_q E_1 I_{o1}\Delta t)(f_1 - f_{ref}) + \delta_{f_{I\sec av}} \\
\dot{f}_2 &= (-1 - K_{Pf\sec} - 2\pi m_q E_2 I_{o2}\Delta t)(f_2 - f_{ref}) + \delta_{f_{I\sec av}} \\
\dot{\delta}_{f_{I\sec av}} &= [-K_{If\sec}(f_1 - f_{ref}) - K_{If\sec}(f_2 - f_{ref})]/2
\end{aligned} \tag{15}$$

Let us define $e_{f1} = f_1 - f_{ref}$ and $e_{f2} = f_2 - f_{ref}$, a state $x_f = \begin{bmatrix} e_{f1} & e_{f2} & \delta_{f_{I\sec av}} \end{bmatrix}^T$, then the system (15) is changed into a linear system

$$\dot{x}_f = A_f x_f. \tag{16}$$

where

$$A_f = \begin{bmatrix} -1 - K_{Pf\sec} - 2\pi m_q E_1 I_{01}\Delta t & 0 & 1 \\ 0 & -1 - K_{Pf\sec} - 2\pi m_q E_2 I_{02}\Delta t & 1 \\ -K_{If\sec}/2 & -K_{If\sec}/2 & 0 \end{bmatrix}.$$

Considering the *Q-f* droop function, the reactive power is dominated by the frequency difference [43], and $E_{1,2}$ can be approximated as constant values in A_f. In addition, $E_{1,2}$ converged to E_{ref} based on the analysis in the former section. Thus, similar to the voltage analysis, (15) is also negative semi-definite if we chose K_{Ifsec}>-1, which means $f_{1,2}$ converge to f_{ref}. Thus, from (15), $\dot{\delta}_{f_{I\sec av}} \equiv 0$, which means that $\delta_{f_{I\sec av}}$ is also stabilized based on LaSalle's theorem [47].

Consequently, the system (16) is also stable. The eigenvalue traces of the system (15) are shown below when various secondary control parameters were selected. The change trend of the eigenvalues is similar to the system (9) in the former section, which further demonstrates that the proposed DAISC will guarantee the stability of the system.

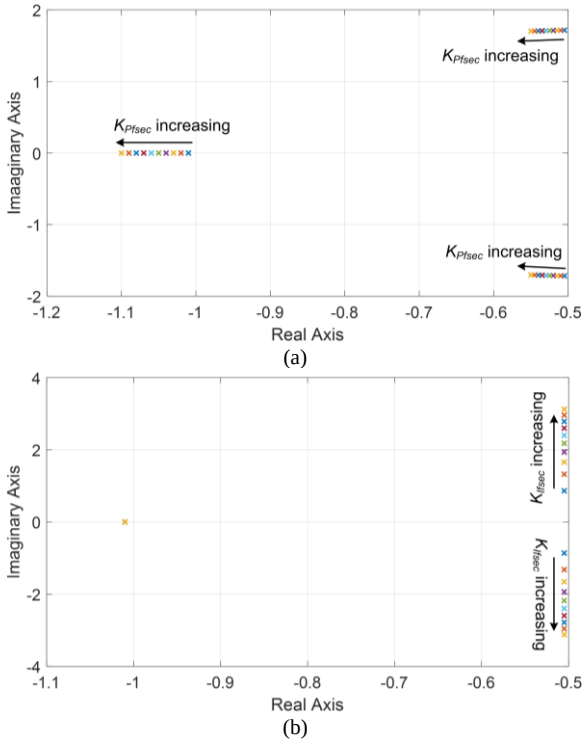

(a)

(b)

Fig. 10. Eigenvalues traces of the system (19). (a) K_{Pfsec} from 0.01 to 0.1, (b) K_{Ifsec} from 1 to 10.

D. Circulating current analysis regarding the power sharing performance

The equivalent circuit of two parallel-connected inverters with virtual impedances is shown in Fig.5, in which Z_{vir1} and Z_{vir2} are the virtual impedances, Z_{line1} and Z_{line2} are the line impedances, E_1 and E_2 are the capacitor voltages to be controlled. I_1 and I_2 are the output currents of the parallel-connected power modules, Z_L is the total load impedance, and I_o is the total load current. Then the circulating current can be defined as follows [14]:

$$I_{cir} = (I_1 - I_2)/2. \tag{17}$$

As shown in Fig. 11, the following equations can be written as:

$$I_1 = \frac{E_1 - E_o}{Z_{vir1} + Z_{line1}} \tag{18}$$

$$I_2 = \frac{E_2 - E_o}{Z_{vir2} + Z_{line2}}. \tag{19}$$

For a sake of simplicity, by assuming that the output impedances of the parallel inverters are equal to each other, $Z_{vir1}+Z_{line1}=Z_{vir2}+Z_{line2}=Z$, then substituting (18)-(19) into (17) gives us:

$$I_{cir} = (E_1 - E_2)/2Z. \tag{20}$$

According to (20), if the output voltages and the output impedances of the parallel inverters are equal to each other

This article has been accepted for publication in a future issue of this journal, but has not been fully edited. Content may change prior to final publication. Citation information: DOI 10.1109/TPEL.2018.2873793, IEEE Transactions on Power Electronics

respectively, the circulating current can be eliminated. Based on the analysis done in Section III.B, C, both of the output voltages E_1 and E_2 will converge to E_{ref}, while the voltage frequency will converge to f_{ref}, which means that circulating current will be suppressed effectively if a proper virtual impedance is selected. In this paper, same virtual impedances are selected since all parallel modules have same power rating. Thus, since the connection line between the converter modules in the modular UPS is quite short, the equivalent output impedances will be very close to each other. The virtual impedances could be different for the applications when the transmission lines are long or when the power ratings are different [47].

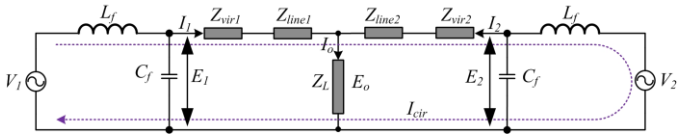

Fig. 11. Equivalent circuit of two parallel inverters with virtual impedances.

IV. Simulation Results

Simulations have been performed in order to verify the proposed DAISC approach. Table I shows the parameters used in the simulations and subsequent experimental results. Two kinds of tests were carried out to verify the static and dynamic performances of the modular UPS system. Figs. 12-14 show the results when module #2 was disconnected and reconnected to the system, thus showing the hot-swap and *plug'n'play* operation capabilities. At 0.15s, module #2 was disconnected from the load; and at 0.8s, it was reconnected again. Compared with the conventional distributed secondary control, a good dynamic performance was obtained, and the power is always average-shared among the parallel modules. It also shows a good transient performance, which is an important index to evaluate the performance of a modular UPS system, especially when critical loads are supplied. From Fig. 14, it also can be seen that windup situation did not happen to the integral controller under the dynamic test.

TABLE I
Main Control and Hardware Parameters in Simulations and Experiments

Coefficient	*Parameters*	*Value*
Nominal output voltage	V_{orms}	230 V
Fundamental frequency	f_o	50 Hz
Filter capacitance	C_f	60 μF
Filter inductance	L_f	200 μH
Virtual impedance	R_{vir1}=R_{vir2}	0.5 Ω
Proportional part of the voltage controller	K_{PV}	0.8 A/V
Resonant part of the voltage controller	K_{RV}	1000 As/V
Proportional part of the current controller	K_{PI}	1.25 V/A
Resonant part of the current controller	K_{RI}	600 Vs/A
Droop coefficient of voltage	m_{p1}=m_{p2}	0.00005 V/W
Droop coefficient of frequency	m_{q1}=m_{q2}	0.00001 Hz/Var
Proportional part of the secondary controller	K_{Psec1}=K_{Psec2}	0.01
Integral part of the secondary controller	K_{Isec1}=K_{Isec2}	3.2

Another dynamic test was performed by making load-step changes, from 0.5 *p.u.* to 1 *p.u.* and vice versa. The first step is at 0.15 s, the load power changed from 0.5 *p.u.* to 1 *p.u.*; and the second step is at 0.4s, back to 0.5 *p.u.* The results are shown in Figs. 15-18. It is worth noting that a good dynamic performance during the transient time is obtained along with an excellent average power sharing performance. Note that the output-voltage frequency did not change much during the transient time as shown in Fig. 18.

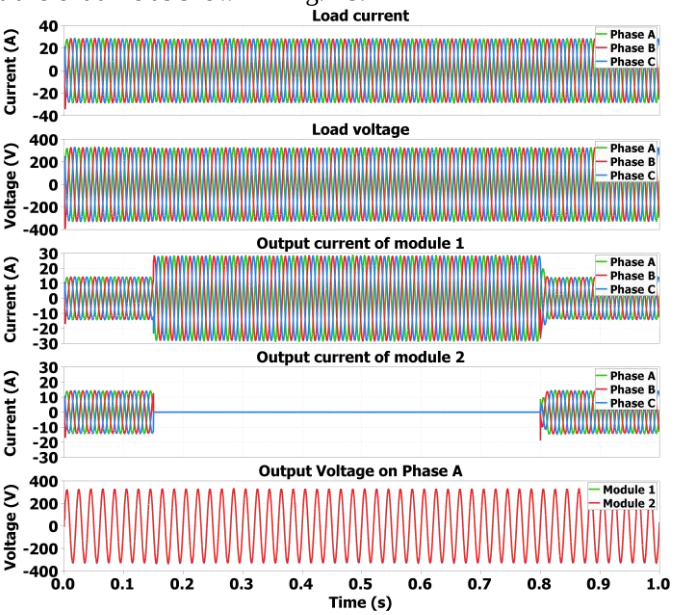

Fig. 12. Simulation results with the proposed distributed secondary control.

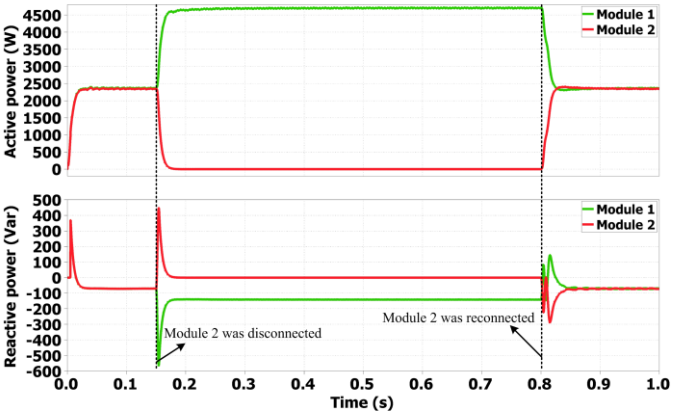

Fig. 13. Output active and reactive powers.

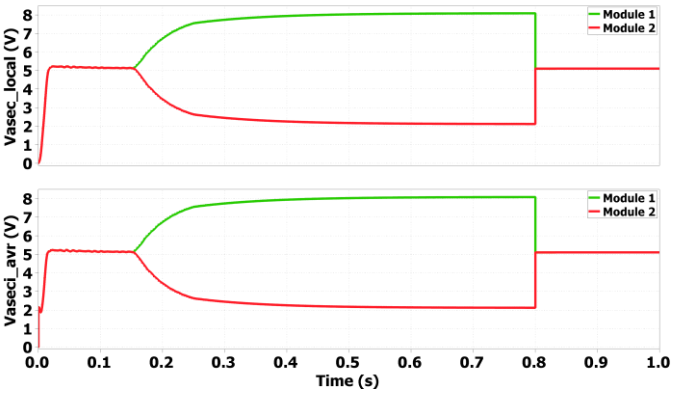

Fig. 14. Local and average values of the integral part of the secondary controller.

This article has been accepted for publication in a future issue of this journal, but has not been fully edited. Content may change prior to final publication. Citation information: DOI 10.1109/TPEL.2018.2873793, IEEE Transactions on Power Electronics

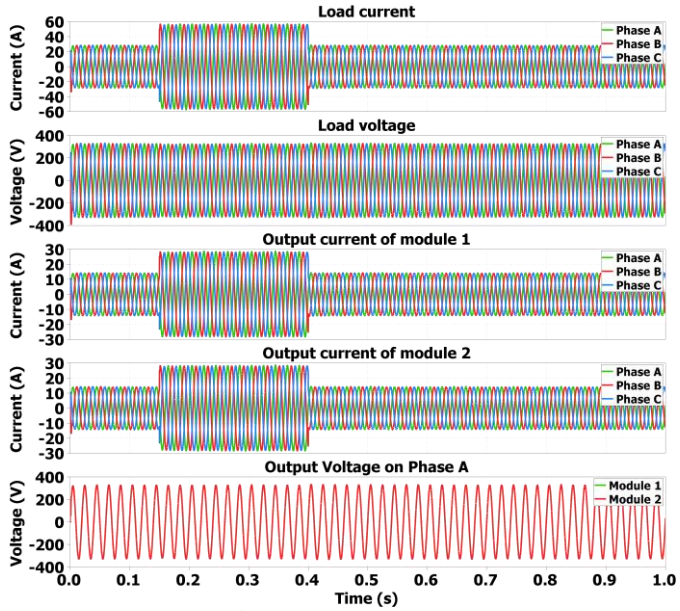

Fig. 15. Simulation results for load-step changes.

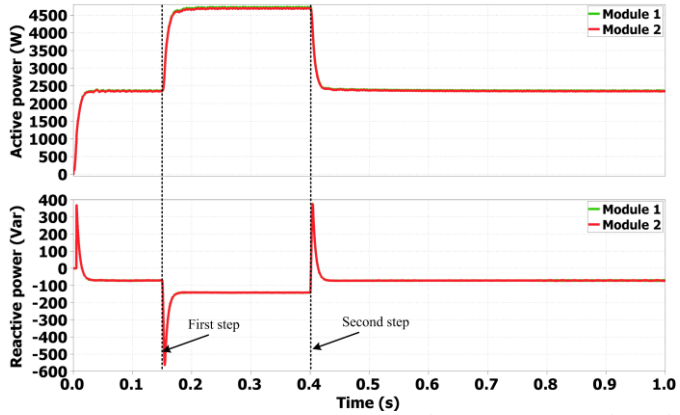

Fig. 16. Active and reactive powers on phase A of the two modules in front of load-step changes.

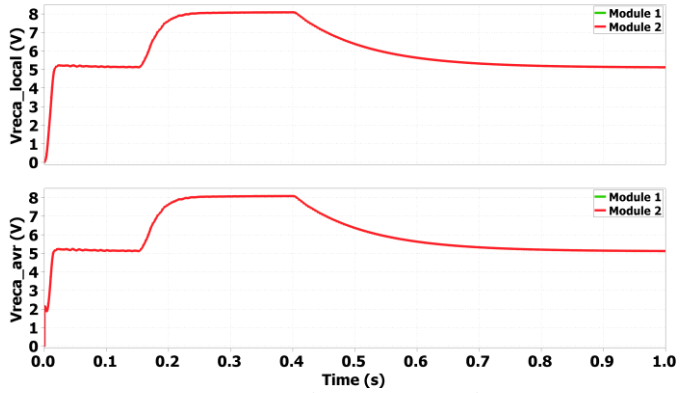

Fig. 17. Local and average values of the integral part of the secondary controller.

V. Experimental Results

The proposed control method aims to be applied in a modular UPS project of cooperation between the Microgrids Research Programme of the Energy Technology Department in Aalborg University [49] and the company Salicru in Barcelona that produces UPS systems [50]. The modular UPS project is named TROY [51] which is based on three-level three-phase NPC inverter. So, the effectiveness of the proposed DAISC strategy was verified by doing experiments on a real modular UPS system. The modular UPS platform is shown in Fig. 19. In order to show the configuration of the system clearly, Fig. 20 shows a simplified diagram of the modular UPS. In each module, it contains its own control unit, AC/DC and DC/AC converters, and an output relay connected to the load. There is a CAN interface in each control unit so that all the modules can communicate with each other through a CAN bus.

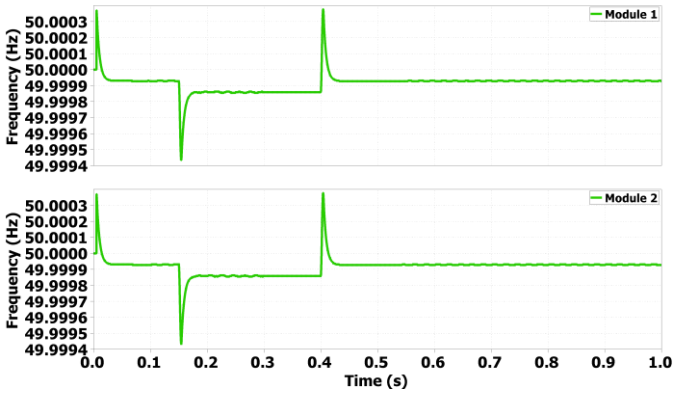

Fig. 18. Output frequency of the two modules.

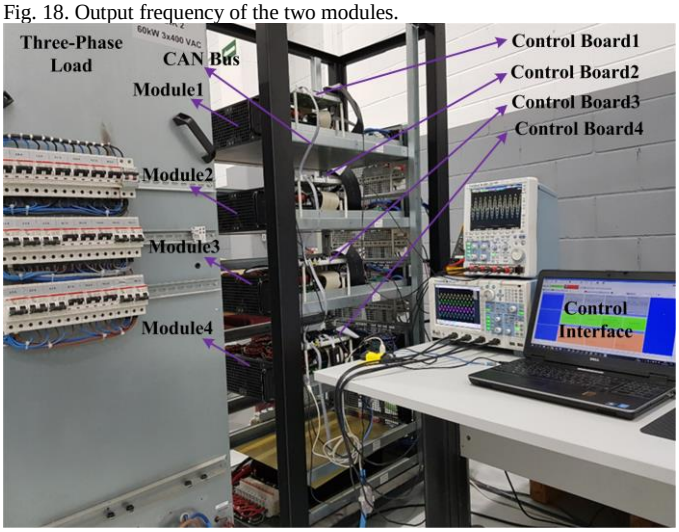

Fig. 19. Modular UPS experimental platform.

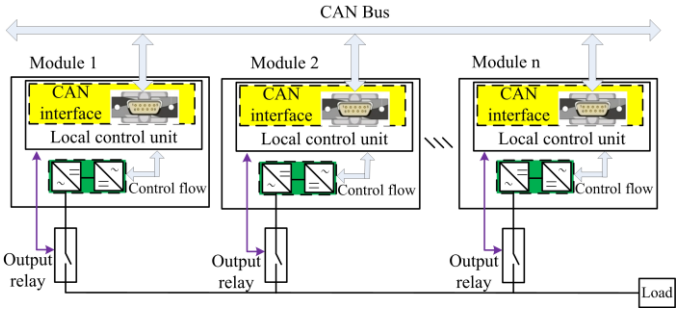

Fig. 20. Simplified diagram of the modular UPS system.

Two kinds of dynamic test were considered in the experiments. In one condition, a constant load was applied, one of the modules will be disconnected and reconnected to the system (hot swap test). Another one is the step load dynamic test, during the test, all the modules are always connected to the load. A most serious condition is considered as well, the outputs

This article has been accepted for publication in a future issue of this journal, but has not been fully edited. Content may change prior to final publication. Citation information: DOI 10.1109/TPEL.2018.2873793, IEEE Transactions on Power Electronics

of the modules are connected directly, one module can be seen as a load of the other one. In addition, four modules under parallel operation is tested to further verify the power sharing and voltage recovery performance when applying the proposed DAISC. Finally, experimental results with capacitive and inductive loads are presented to further show the effectiveness of the proposed method for different kinds of load.

From the experimental results of the proposed distributed secondary control on the real commercial modular UPS platform, the average power sharing performance of the UPS system can always be guaranteed; the voltage and frequency can always be stable under dynamic test with both resistive, inductive and capacitive loads as well. It means that voltage and frequency of each module can always be recovered and synchronized, or the safety of parallel operation of a modular UPS can be guaranteed.

A. Operation of CAN bus communication

A low bandwidth CAN communication is used in the control, the data sharing through the CAN bus is updated every 20ms, a fundamental cycle. The detail of the CAN communication setup is shown in Table II. It should be noticed that, one frame stands for one data sending, the frame length is 108 bits, in which 64 bits is for the data itself, the other 44 bits is for the CAN configuration of how to handle this data like the identifying of the datas.

In the modular UPS platform, the modules have their own physical IDs. In the control configuration, the module with lower physical ID has priority to send data to the CAN bus, once the module receives a data, it will be stored in the register. When all the modules finish the work of data sending, each module will obtain the average value of power in their own digital controller.

TABLE II CONFIGURATION OF THE CAN BUS

Parameters	Value
Bit rate	500kbps
Frame length	44 (bits data handling) + 64 (bits data) = 108 bits
Frame rate	500kbps/108bits = 4629.629
Frame time	1/4629.629 =216μs
1 data sending time	216μs

B. Plug'and'play performance test

Fig. 21 shows the voltage and current waveforms of the two modules in steady state. The output currents are almost the same, a good average power sharing performance is obtained. Fig. 22 shows the waveforms during the transient time when one module was disconnected from the system, the steady state waveform is shown in Fig. 23. Fig. 24 shows the waveforms during the transient time when module #2 was reconnected to the load, the steady state waveforms is shown in Fig. 25. From the experimental results, a good dynamic performance is obtained, the power can always be averagely shared under parallel operation.

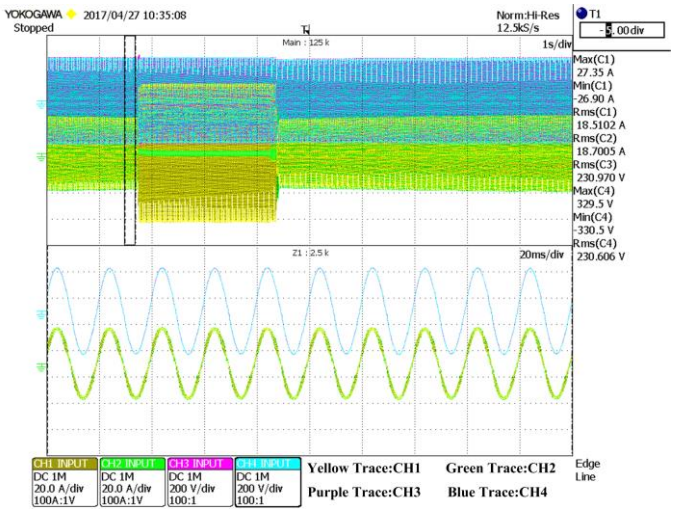

Fig. 21. Waveforms of voltage and current at steady state, CH1: Phase A current of module #1; CH2: Phase A current of module #2; CH3: Phase A voltage of module #1; CH4: Phase A voltage of module #2.

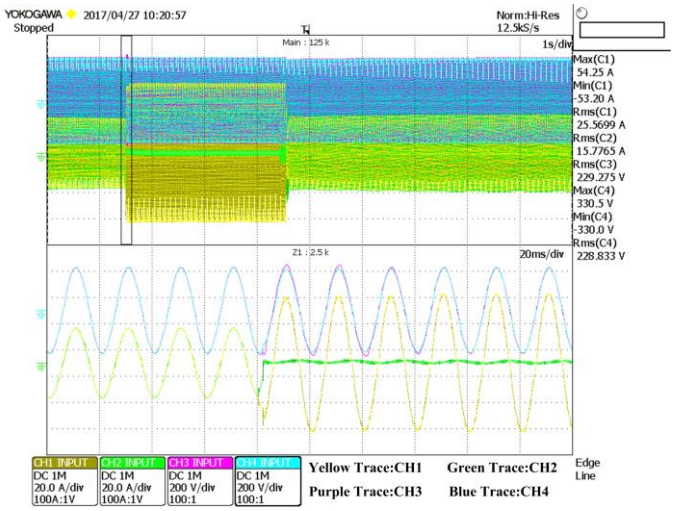

Fig. 22. Waveforms during the transient time when module #2 was disconnected from the system, CH1: Phase A current of module #1; CH2: Phase A current of module #2; CH3: Phase A voltage of module #1; CH4: Phase A voltage of module #2.

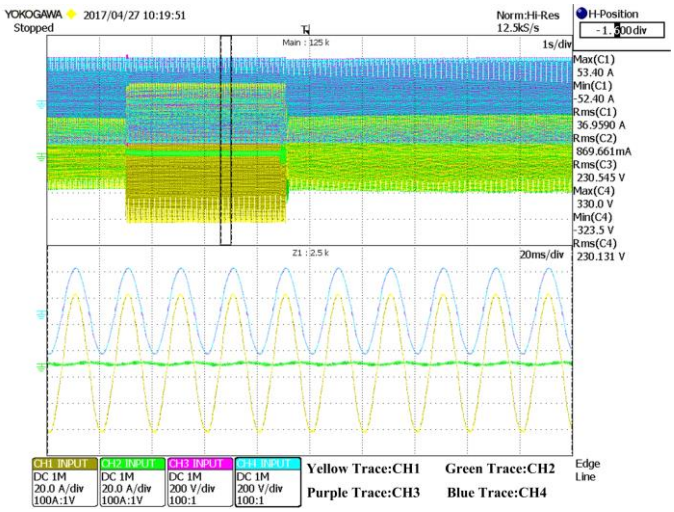

Fig. 23. Waveforms at the steady state after module #2 was disconnected, CH1: Phase A current of module #1; CH2: Phase A current of module #2; CH3: Phase A voltage of module #1; CH4: Phase A voltage of module #2.

This article has been accepted for publication in a future issue of this journal, but has not been fully edited. Content may change prior to final publication. Citation information: DOI 10.1109/TPEL.2018.2873793, IEEE Transactions on Power Electronics

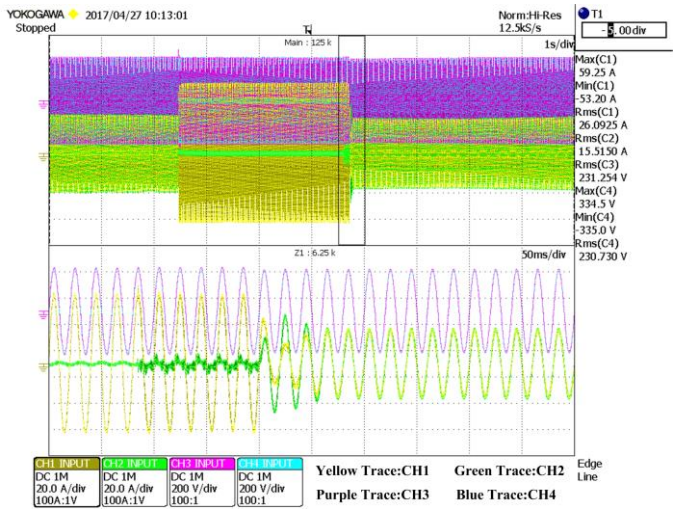

Fig. 24. Waveforms during the transient time when module #2 was reconnected to the system, CH1: Phase A current of module #1; CH2: Phase A current of module #2; CH3: Phase A voltage of module #1; CH4: Phase A voltage of module #2.

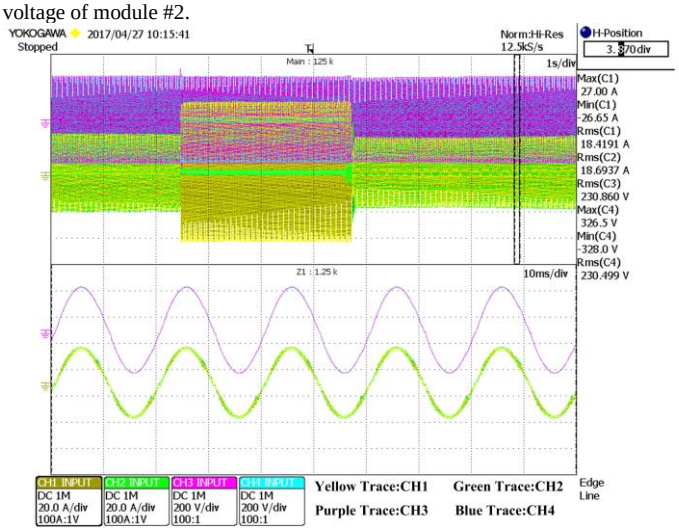

Fig. 25. Waveforms of voltage and current at steady state after the dynamic test with proposed distributed secondary control, CH1: Phase A current of module #1; CH2: Phase A current of module #2; CH3: Phase A voltage of module #1; CH4: Phase A voltage of module #2.

C. Load-step changes dynamic test

In the experiments, the step load was configured as: stepped from 1 *p.u.* to 0.5 *p.u.*, then stepped back. The experimental results are shown in Figs. 26 and 27. The currents can always be averagely shared among the two modules along with a stable output voltage. Fig. 28 shows the results when the output terminals of the two modules were directly connected to each other suddenly, which is a serious occasion for the modules under parallel operation. It shows a good current balance performance, there was no serious negative current flowing from one module to another, which will guarantee the safety of the DC link of each module, and it is also an important point to evaluate the reliability of a modular UPS.

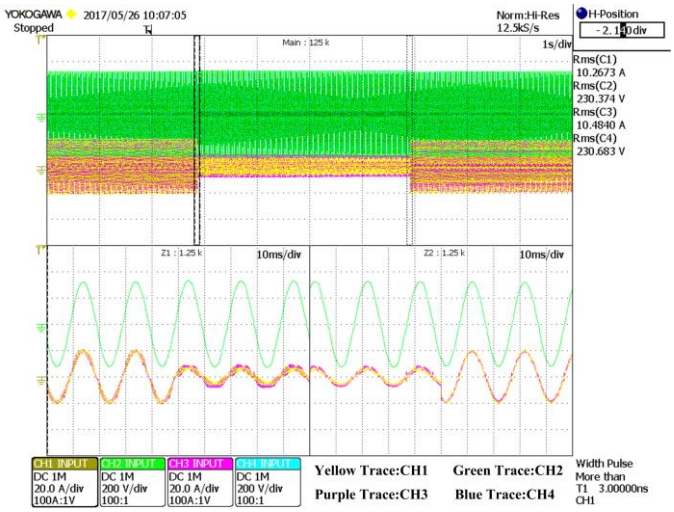

Fig. 26. Experimental results during the transient time with step load, CH1: Phase A current of module #1; CH2: Phase A voltage of module #1; CH3: Phase A current of module #2; CH4: Phase A voltage of module #2.

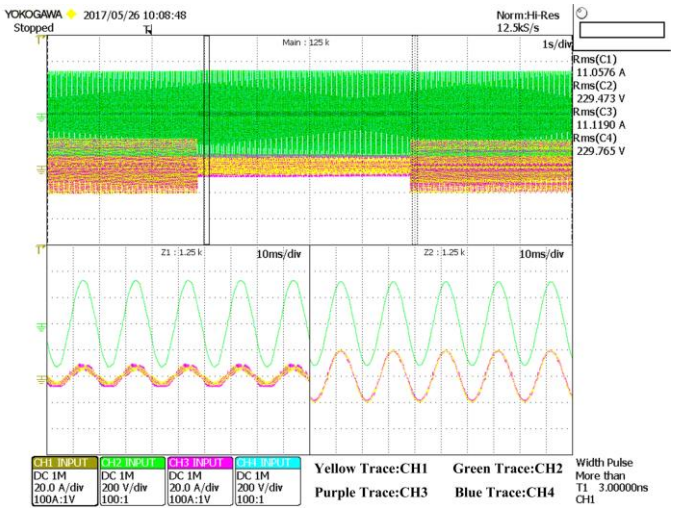

Fig. 27. Experimental results under steady state with step load, CH1: Phase A current of module #1; CH2: Phase A voltage of module #1; CH3: Phase A current of module #2; CH4: Phase A voltage of module #2.

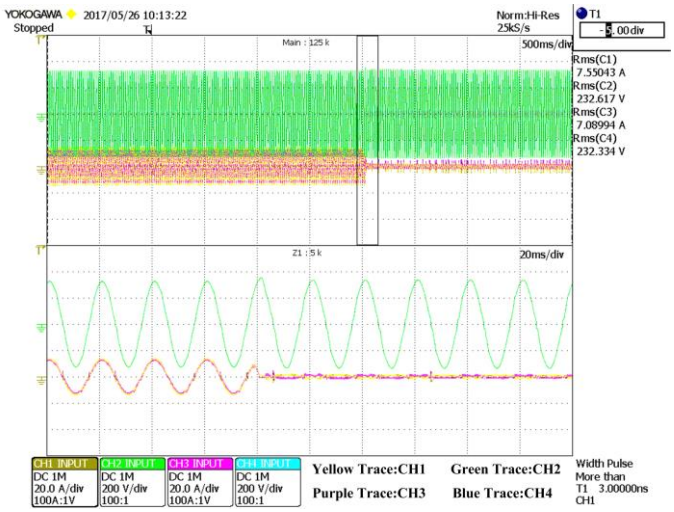

Fig. 28. Dynamic test when the output terminals of the modules were directly connected, CH1: Phase A current of module #1; CH2: Phase A voltage of module #1; CH3: Phase A current of module #2; CH4: Phase A voltage of module #2.

This article has been accepted for publication in a future issue of this journal, but has not been fully edited. Content may change prior to final publication. Citation information: DOI 10.1109/TPEL.2018.2873793, IEEE Transactions on Power Electronics

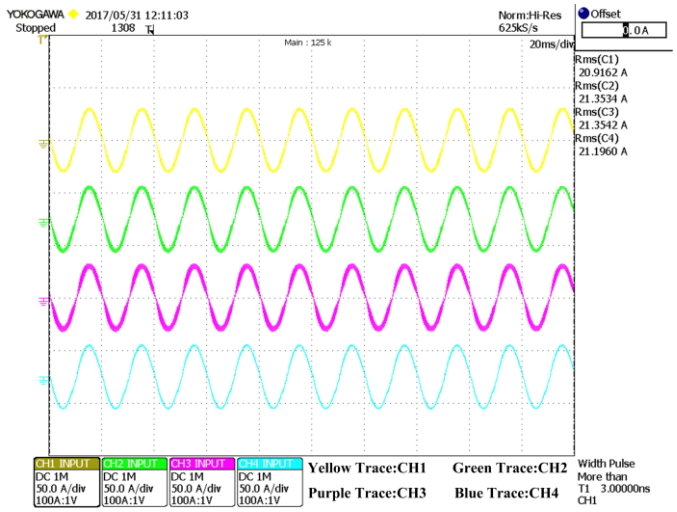

Fig. 29. Current waveforms when four modules in parallel operation, CH1: Phase A current of module #1; CH2: Phase A current of module #2; CH3: Phase A current of module #3; CH4: Phase A current of module #4.

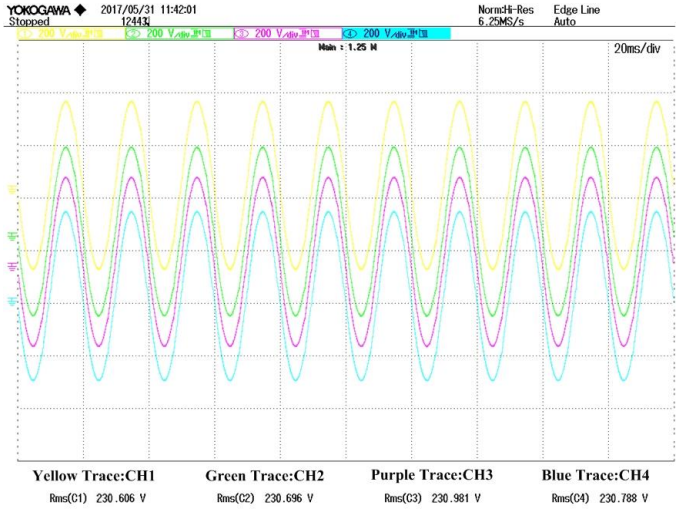

Fig. 30. Voltage waveforms when four modules in parallel operation, CH1: Phase A voltage of module #1; CH2: Phase A voltage of module #2; CH3: Phase A voltage of module #3; CH4: Phase A voltage of module #4.

Moreover, four modules in parallel operation was tested, Figs. 29 and 30 show the current and voltage waveforms of the phase A of the four modules, respectively. It can be seen that the current can approximated averagely shared among the four modules, and the voltage is recovered to the reference value at the same time, which further verify the effectiveness of the proposed DAISC.

D. Capacitive and inductive loads tests

In order to further show the effectiveness of the proposed method, experiments when capacitive or inductive load are connected have been developed individually. The load is suddenly disconnected to the modular UPS system at the time t_x, Fig. 31 shows the results when a capacitive load is connected, while the result of inductive load is depicted in Fig. 32. From these results, it can be found that the load current can always be average shared between the parallel connected power modules, which demonstrates that the proposed method is valid for both resistive, inductive and capacitive loads. Thus, the proposed control strategy can ensure average power sharing as well as the nominal output voltage and frequency independently from active/reactive power load nature.

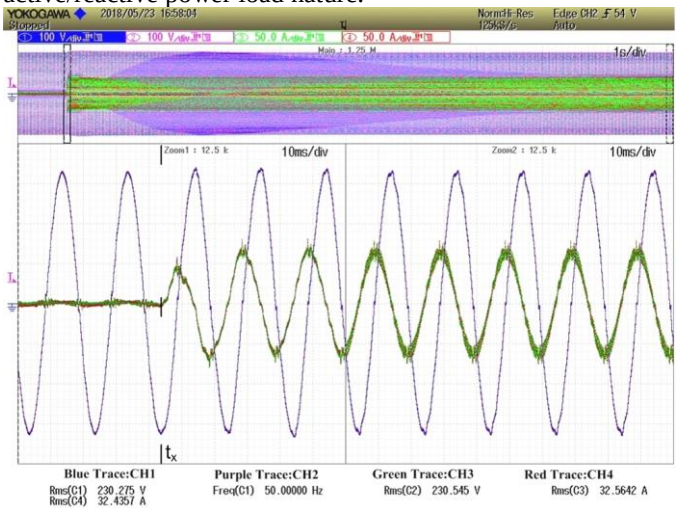

Fig. 31. Experimental results when capacitive load is connected. CH1: Phase A voltage of module #1; CH2: Phase A voltage of module #2; CH3: Phase A current of module #1; CH4: Phase A current of module #2.

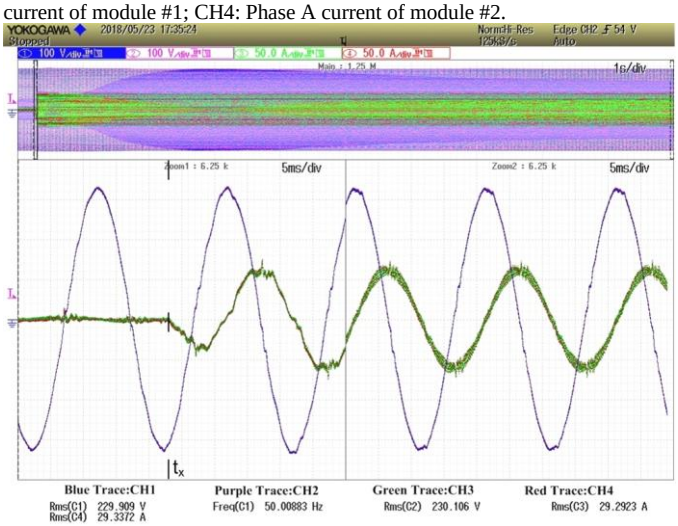

Fig. 32. Experimental results when inductive load is connected. CH1: Phase A voltage of module #1; CH2: Phase A voltage of module #2; CH3: Phase A current of module #1; CH4: Phase A current of module #2.

VI. CONCLUSION

In this paper, a novel distributed secondary control (DAISC) is proposed for modular UPS systems. Compared with the existing distributed secondary control, it improves the dynamic performance of the parallel operation of converter modules. An excellent power sharing performance is obtained, which is an important requirement for a modular UPS system, and at the same time it can ensure nominal output voltage and frequency. Further, stability analysis is presented to verify the availability of the DAISC. The performance of the improved distributed secondary control was verified with both simulations using PLECS and experimental results on a real modular UPS system under different dynamic scenarios with resistive, capacitive and inductive loads.

ACKNOWLEDGMENT

This work was supported by the cooperation project between Aalborg University and the company Salicru S.A. The authors

would like to thanks to colleagues Jordi Montero, Ramon Pinyol, Ramon Ciurans, Daniel Revilla, and Andreu Sabe from Salicru for their help and support.

REFERENCES

[1] P. Wang, X. Lu, X. Yang, W. Wang and D. Xu, "An Improved Distributed Secondary Control Method for DC Microgrids With Enhanced Dynamic Current Sharing Performance," *IEEE Trans. Power Electron.*, vol. 31, no. 9, pp. 6658-6673, Sept. 2016.

[2] R. Lasseter, A. Akhil, C. Marnay, J. Stevens, J. Dagle, R. Guttromson, A. Meliopoulous, R. Yinger, and J. Oto, "The certs microgrid concept-White paper on integration of distributed energy resources," U.S. Dept. Energy, Lawrence Berkeley Nat. Lab., Berkeley, CA, USA, Tech. Rep. LBNL-50829, 2002.

[3] J. M. Guerrero, J. C. Vasquez, L. G. Vicuña, and M. Castilla, "Hierarchical Control of Droop-Controlled AC and DC Microgrids—A General Approach Toward Standardization," *IEEE Trans. Ind. Electron*., vol. 58, no. 1, pp. 158–172, Jan. 2011.

[4] J. A. Pecas Lopes, C. L. Moreira and A. G. Madureira, "Defining control strategies for microgrids islanded operation," *IEEE Trans. Power Syst*., vol. 21, no. 2, pp. 916-924, May, 2006.

[5] J. M. Guerrero, M. Chandorkar, T. Lee and P. C. Loh, "Advanced control architechtures for intelligent microgrids-part I: decentralized and hierarchical control," *IEEE Trans. Ind. Electron*., vol. 60, no. 4, pp. 1254- 1262, Apr., 2013.

[6] F. Blaabjerg, R. Teodorescu, M. Liserre and A. V. Timbus, "Overview of control and grid synchronization for distributed power generation systems," *IEEE Trans. Ind. Electron*., vol. 53, no. 5, pp. 1398-1409, Oct., 2006.

[7] J. M. Guerrero, P. C. Loh, T. Lee and M. Chandorkar, "Advanced control architechtures for intelligent microgrids-part II: power quality, energy storage, and AC/DC microgrids," *IEEE Trans. Ind. Electron*., vol. 60, no. 4, pp. 1263-1270, Apr., 2013.

[8] J. W. Simpson-Porco, F. Dorfler, and F. Bullo, "Synchronization and power sharing for droop-controlled inverters in islanded microgrids," *Automatica*, vol. 49, no. 9, pp. 2603-2611, Sep., 2013.

[9] M. Yazdanian and A. Mehrizi-Sani, "Distributed control techniques in microgrids," *IEEE Trans. Smart Grid*, vol. 5, no. 6, pp. 2901-2909, Nov., 2014.

[10] M. H. Nazari, Z. Costello, M. J. Feizollahi, S. Grijalva, and M. Egerstedt, "Distributed frequency control of prosumer-based electric energy systems," *IEEE Trans. Power Syst*., vol. 29, no. 6, pp. 2934-2942, Nov., 2014.

[11] H. Cai, G. Hu, F. L. Lewis, A. Davoudi, "A distributed feedforward approach to cooperative control of AC microgrids," *IEEE Trans. Power Syst*., vol. 31, no. 5, pp. 4057-4067, 2016.

[12] D. C. Pham, S. Huang, and K. Huang, "Modeling and Simulation of Current Source Inverters with Space Vector Modulation," in *Proc. IEEE ICEMS* 2010, Oct. 10-13, pp. 320 - 325.

[13] X. Zhang, Z. Wang, and S. Zhou, "How to ensure the modular UPS with high reliability," in *Proc. IEEE INTELEC* 2015, Oct. 18-22, pp. 1 - 4.

[14] J. M. Guerrero, L. G. Vicuña, J. Matas, M. Castilla, and J. Miret, "Output Impedance Design of Parallel-Connected UPS Inverters With Wireless Load-Sharing Control," *IEEE Trans. Ind. Electron*., vol. 52, no. 4, pp. 1126–1135, Aug. 2005.

[15] C. Zhang, J. M. Guerrero, J. C. Vasquez and C. M. Seniger, "Modular Plug'n'Play Control Architectures for Three-Phase Inverters in UPS Applications," in *IEEE Trans. Ind. Appl.*, vol. 52, no. 3, pp. 2405-2414, May-June 2016.

[16] B. Zhao, Q. Song, W. Liu and Y. Xiao, "Next-Generation Multi-Functional Modular Intelligent UPS System for Smart Grid," *IEEE Trans. Ind. Electron*., vol. 60, no. 9, pp. 3602-3618, Sept. 2013.

[17] Yu Zhang, Mi Yu, Fangrui Liu, Shuming Li, Jianwei Wang and Yong Kang, "Instantaneous current share method for modular UPS through virtual impedance," *37th Annual Conference of the IEEE Industrial Electronics Society* (IECON), Melbourne, VIC, 2011, pp. 1384-1389.

[18] L. Saro, and C. Zanettin, "The impact of a single module's MTBF value in modular UPS systems: Technique for its assessment, improvement and final validation," in *Proc. IEEE INTELEC* 2016, Oct. 23-27, pp. 1 - 8.

[19] J. M. Guerrero, J. Matas, L. G. Vicuna, M. Castilla, and J. Miret, "Wireless-control strategy for parallel operation of distributed-generation inverters," *IEEE Trans. Ind. Electron*., vol. 53, no. 5, pp. 1461–1470, Oct. 2006.

[20] Y. Zhang, M. Yu, F. Liu, and Y. Kang, "Instantaneous Current-Sharing Control Strategy for Parallel Operation of UPS Modules Using Virtual Impedance," *IEEE Trans. Power Electron*., vol. 28, no. 1, pp. 432-440, Jan. 2013.

[21] H. Cai; G. Hu, "Distributed Nonlinear Hierarchical Control of AC Microgrid via Unreliable Communication," *IEEE Trans. Smart Grid*, vol.PP, no.99, pp.1-1.

[22] H. Cai and G. Hu, "Consensus-based distributed nonlinear hierarchical control of AC microgrid under switching communication network," *12th IEEE International Conference on Control and Automation* (ICCA), Kathmandu, 2016, pp. 571-576.

[23] B. Wei, Y. Yuehao, C. Yuanhong and B. Weiyu, "An hierarchical control of AC microgrid composed of distributed power resources based on voltage source converter," *IEEE Innovative Smart Grid Technologies - Asia* (ISGT ASIA), Bangkok, 2015, pp. 1-6.

[24] G. Lou, W. Gu, Y. Xu, M. Cheng and W. Liu, "Distributed MPC-Based Secondary Voltage Control Scheme for Autonomous Droop-Controlled Microgrids," *IEEE Trans. Sus. Energy*, vol. 8, no. 2, pp. 792-804, April 2017.

[25] A. Bidram, F. L. Lewis and A. Davoudi, "Distributed Control Systems for Small-Scale Power Networks: Using Multiagent Cooperative Control Theory," *IEEE Control Systems*, vol. 34, no. 6, pp. 56-77, Dec. 2014.

[26] A. Bidram and A. Davoudi, "Hierarchical structure of microgrids control system," *IEEE Trans. Smart Grid*, vol. 3, pp. 1963–1976, Dec. 2012.

[27] N. Pogaku, M. Prodanovic, and T. C. Green, "Modeling, analysis and testing of autonomous operation of an

inverter-based microgrid," *IEEE Trans. Power Electron*., vol. 22, no. 2, pp. 613–625, Mar. 2007.

[28] J. A. Pecas Lopes, C. L. Moreira, and A. G. Madureira, "Defining control strategies for microgrids islanded operation," *IEEE Trans. Power Syst*., vol. 21, no. 2, pp. 916–924, May 2006.

[29] J. C. Vasquez, J. M. Guerrero, M. Savaghebi, J. Eloy-Garcia, and R. Teodorescu, "Modeling, analysis and design of stationary-referenceframe droop-controlled parallel three-phase voltage source inverters," *IEEE Trans. Ind. Electron*., vol. 60, no. 4, pp. 1271–1280, Apr. 2013.

[30] P. H. Divshali, A. Alimardani, S. H. Hosseinian, and M. Abedi, "Decentralized cooperative control strategy of microsources for stabilizing autonomous VSC-based microgrids," *IEEE Trans. Power Syst*., vol. 27, no. 4, pp. 1949–1959, Nov. 2012.

[31] Q. C. Zhong, "Robust droop controller for accurate proportional load sharing among inverters operated in parallel," *IEEE Trans. Ind. Electron*., vol. 60, no. 4, pp. 1281–1290, Apr. 2013.

[32] J. M. Guerrero, J. C. Vasquez, J. Matas, M. Castilla, and L. G. de Vicuna, "Control strategy for flexible microgrid based on parallel line-interactive UPS systems," *IEEE Trans. Ind. Electron*., vol. 56, no. 3, pp. 726–736, Mar. 2009.

[33] D. E. Olivares et al., "Trends in microgrid control," *IEEE Trans. Smart Grid*, vol. 5, no. 4, pp. 1905–1919, Jul. 2014.

[34] M. Savaghebi, A. Jalilian, J. Vasquez, and J. Guerrero, "Secondary control scheme for voltage unbalance compensation in an islanded droop-controlled microgrids," *IEEE Trans. Smart Grid*., vol. 3, no. 11, pp. 7025–7038, Nov. 2015.

[35] J. Y. Kim et al., "Cooperative control strategy of energy storage system and microsources for stabilizing the microgrid during islanded operation," *IEEE Trans. Power Electron*., vol. 25, no. 12, pp. 3037–3048, Dec. 2010.

[36] A. Mehrizi-Sani and R. Iravani, "Potential-function based control of a microgrid in islanded and grid-connected models," *IEEE Trans. Power Syst*., vol. 25, no. 4, pp. 1883–1891, Nov. 2010.

[37] Q. Shafiee, J. M. Guerrero, and J. C. Vasquez, "Distributed secondary control for islanded microgrids- A novel approach," *IEEE Trans. Power Electron*., vol. 29, no. 2, pp. 1018–1031, Feb. 2014.

[38] A. Villa, F. Belloni, R. Chiumeo and C. Gandolfi, "Conventional and reverse droop control in islanded microgrid: Simulation and experimental test," *International Symposium on Power Electronics, Electrical Drives, Automation and Motion* (SPEEDAM), Anacapri, 2016, pp. 288-294.

[39] Dan Wu, Fen Tang, J. C. Vasquez and J. M. Guerrero, "Control and analysis of droop and reverse droop controllers for distributed generations," *IEEE 11th International Multi-Conference on Systems, Signals & Devices* (SSD14), Barcelona, 2014, pp. 1-5.

[40] J. He, and Y. W. Li, "Analysis and design of interfacing inverter output virtual impedance in a low voltage microgrid," in *Proc 2010, Energy Conv. Cong. and Exp. (ECCE)*, pp. 2857–2864.

[41] M. Savaghebi, J. C. Vasquez, A. Jalilian, J. M. Guerrero, and T. Lee , "Selective Harmonic Virtual Impedance for Voltage Source Inverters with LCL filter in Microgrids," in *Proc 2012, Energy Conv. Cong. and Exp. (ECCE)*, Sept. 15-20, Raleigh, NC, USA, pp. 1960–1965.

[42] J. C. Vasquez, J. M. Guerrero, M. Savaghebi, J, Eloy-Garcia, and R. Teodorescu, "Modeling, Analysis, and Design of Stationary Reference Frame Droop Controlled Parallel Three- Phase Voltage Source Inverters," *IEEE Trans. Ind. Electron*., vol. 60, no. 4, pp. 1271–1280, Apr. 2013.

[43] J. Matas, M. Castilla, L. Vicuña, J. Miret, and J. C. Vasquez, "Virtual Impedance Loop for Droop-Controlled Single-Phase Parallel Inverters Using a Second-Order General-Integrator Scheme," *IEEE Trans. Power Electron*., vol. 25, no. 12, pp. 2993–3001, Dec. 2010.

[44] J. W. Simpson-Porco, Q. Shafiee, F. Dörfler, J. C. Vasquez, J. M. Guerrero and F. Bullo, "Secondary Frequency and Voltage Control of Islanded Microgrids via Distributed Averaging," *IEEE Trans. Ind. Electron.*, vol. 62, no. 11, pp. 7025-7038, Nov. 2015.

[45] C. K. Sao, and P. W. Lehn, "Autonomous load sharing of voltage source converters," IEEE Trans. Power Del., vol. 20, no. 2, pp. 1009–1016, Apr. 2005.

[46] J. M. Guerrero, J. Matas, L. G. Vicuña, M. Castilla, and J. Miret, " Decentralized Control for Parallel Operation of Distributed Generation Inverters Using Resistive Output Impedance," *IEEE Trans. Ind. Electron.*, vol. 54, no. 2, pp. 994-1004, Apr. 2007.

[47] H. Khalil, "Nonlinear Systems," 3rd ed. Prentice Hall, 2002.

[48] J. M. Guerrero, L. Hang, J. Uceda, "Control of distributed uninterruptible power supply systems," *IEEE Trans. Ind. Electron*., vol. 55, no. 8, pp. 2845-2859, Jul.. 2008.

[49] Microgrids Research Programme: www.microgrids.et.aau.dk

[50] Salicru S.A.: www.salicru.com/en

[51] Troy project: www.troy.et.aau.dk

Baoze Wei (S'15-M'18) received the B.S. degree in electrical engineering, the M.S. degree in power electronics and power drives from Yanshan University, Qinhuangdao, China, and the Ph.D. degree in power electronic systems from the Department of Energy Technology, Aalborg University, Aalborg, Denmark, in 2010, 2014, and 2017, respectively. He is currently working in the Department of Energy Technology, Aalborg University as a postdoctoral researcher.

His research interests include microgrid, modular power inverters for uninterruptible power system, photovoltaic generation system, paralleling power converter for renewable generation systems, power quality, as well as the applications of distributed control.

Yonghao Gui (S'11-M'17) received the B.S. degree in automation from Northeastern University, Shenyang, China, in 2009. He received the M.S. and Ph.D. degrees in electrical engineering from Hanyang University, Seoul, South Korea, in 2012 and 2017, respectively.

Since Feb. 2017, he has been working with the Department of Energy Technology, Aalborg University, Denmark, where he is a Postdoctoral Researcher. His research interests include control of power electronics in power systems

This article has been accepted for publication in a future issue of this journal, but has not been fully edited. Content may change prior to final publication. Citation information: DOI 10.1109/TPEL.2018.2873793, IEEE Transactions on Power Electronics

Albert Marzàbal received the B.S. degree in telecommunications engineering, the M.S. degree in electronics engineering (with the highest distinction), and the diploma of advanced studies (DEA) in the PhD program of Vision, Control and Robotics from the Technical University of Catalonia, Barcelona, Catalonia, in 2000, 2005, and 2009, respectively.

He currently works in the research laboratory of Salicru, S.A., a company that has designed, manufactured and commercialised power electronics products for the key sectors of the energy market since 1965. He has some publications and he worked as developer at Institut de Robòtica i Informàtica Industrial , and as professor in engineering topics at Technical University of Catalonia 10 years.

Santi Trujillo was born in Catalonia on 1979. He received the B.S. degree in industrial technical engineering, specialty in industrial electronics, from the Industrial Technical Engineering University of Barcelona, Barcelona, Catalonia, in 2002.

Since 1999 he has been with Salicru, S.A., Palautordera, Spain, where he is currently the magnetics chief engineer and an assistant control engineer in the research laboratory.

Josep M. Guerrero (S'01-M'04-SM'08-FM'15) received the B.S. degree in telecommunications engineering, the M.S. degree in electronics engineering, and the Ph.D. degree in power electronics from the Technical University of Catalonia, Barcelona, in 1997, 2000 and 2003, respectively. Since 2011, he has been a Full Professor with the Department of Energy Technology, Aalborg University, Denmark, where he is responsible for the Microgrid Research Program (www.microgrids.et.aau.dk). From 2012 he is a guest Professor at the Chinese Academy of Science and the Nanjing University of Aeronautics and Astronautics; from 2014 he is chair Professor in Shandong University; from 2015 he is a distinguished guest Professor in Hunan University; and from 2016 he is a visiting professor fellow at Aston University, UK, and a guest Professor at the Nanjing University of Posts and Telecommunications.

His research interests is oriented to different microgrid aspects, including power electronics, distributed energy-storage systems, hierarchical and cooperative control, energy management systems, smart metering and the internet of things for AC/DC microgrid clusters and islanded minigrids; recently specially focused on maritime microgrids for electrical ships, vessels, ferries and seaports. Prof. Guerrero is an Associate Editor for a number of IEEE TRANSACTIONS. He received the best paper award of the IEEE Transactions on Energy Conversion for the period 2014-2015, and the best paper prize of IEEE-PES in 2015. As well, he received the best paper award of the Journal of Power Electronics in 2016. In 2014, 2015, 2016, and 2017 he was awarded by Thomson Reuters as Highly Cited Researcher. In 2015 he was elevated as IEEE Fellow for his contributions on "distributed power systems and microgrids."

Juan C. Vasquez (M'12-SM'14) received the B.S. degree in electronics engineering from the Autonomous University of Manizales, Manizales, Colombia, and the Ph.D. degree in automatic control, robotics, and computer vision from the Technical University of Catalonia, Barcelona, Spain, in 2004 and 2009, respectively. He was with the Autonomous University of Manizales working as a teaching assistant and the Technical University of Catalonia as a Post-Doctoral Assistant in 2005 and 2008 respectively. In 2011, He was Assistant Professor and from 2014 he is working as an Associate Professor at the Department of Energy Technology, Aalborg University, Denmark where He is the Vice Programme Leader of the Microgrids Research Program (see microgrids.et.aau.dk). He was a Visiting Scholar at the Center of Power Electronics Systems (CPES) at Virginia Tech and a visiting professor at Ritsumeikan University, Japan. His current research interests include operation, advanced hierarchical and cooperative control, optimization and energy management applied to distributed generation in AC/DC Microgrids, maritime microgrids, advanced metering infrastructures and the integration of Internet of Things into the SmartGrid. Dr Vasquez is a Associate Editor of IET POWER ELECTRONICS and a Guest Editor of the IEEE TRANSACTIONS ON INDUSTRIAL INFORMATICS Special Issue on Energy Internet. In 2017, Dr. Vasquez was awarded as Highly Cited Researcher by Thomson Reuters. Dr. Vasquez is currently a member of the IEC System Evaluation Group SEG4 on LVDC Distribution and Safety for use in Developed and Developing Economies, the Renewable Energy Systems Technical Committee TC-RES in IEEE Industrial Electronics, PELS, IAS, and PES Societies.